

Electronic Supplementary Information (ESI)

Polarity assessment of hydroxide mediated P(VDF-TrFE) composites for piezoelectric energy harvesting and self-powered mechanosensing

Abhishek Sasmal^{a,b}, Payel Maiti^c, Arunachalakasi Arockiarajan^{b,d}, Shrabanee Sen^{a,*}

^aFunctional Materials and Devices Division, CSIR-Central Glass & Ceramic Research Institute, Kolkata – 700032, India

^bDepartment of Applied Mechanics and Biomedical Engineering, Indian Institute of Technology Madras (IIT Madras), Chennai, Tamil Nadu – 600036, India

^cDepartment of Metallurgical and Materials Engineering, Indian Institute of Technology Kharagpur (IIT Kharagpur), Kharagpur, West Bengal – 721302, India

^dCentre of Excellence in Ceramics Technologies for Futuristic Mobility, Indian Institute of Technology Madras (IIT Madras), Chennai, Tamil Nadu - 600036, India

*E-mail ID: shrabanee@cgcricri.res.in

Fig. S1

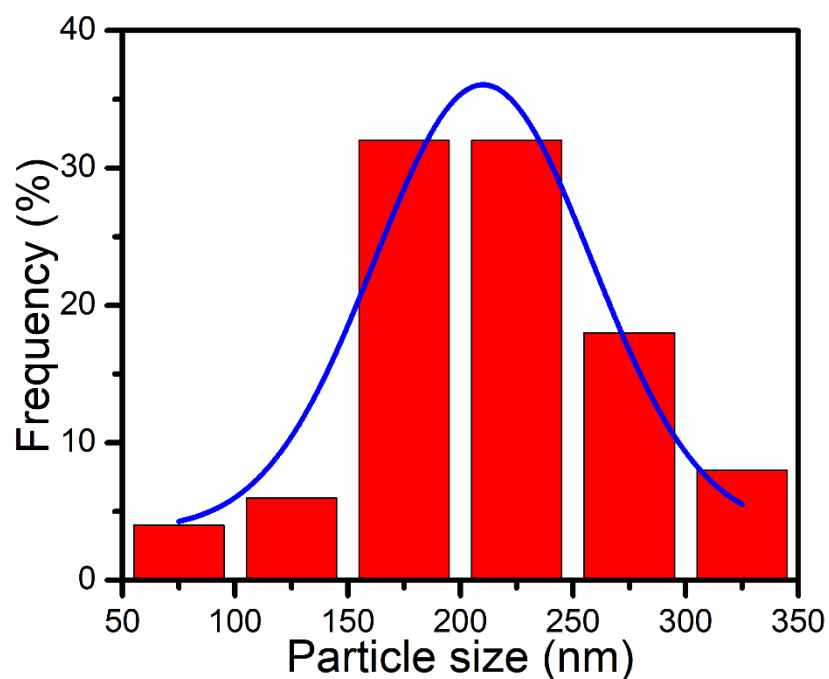


Fig. S1. Size distribution of the synthesized ZS particles.

Fig. S2

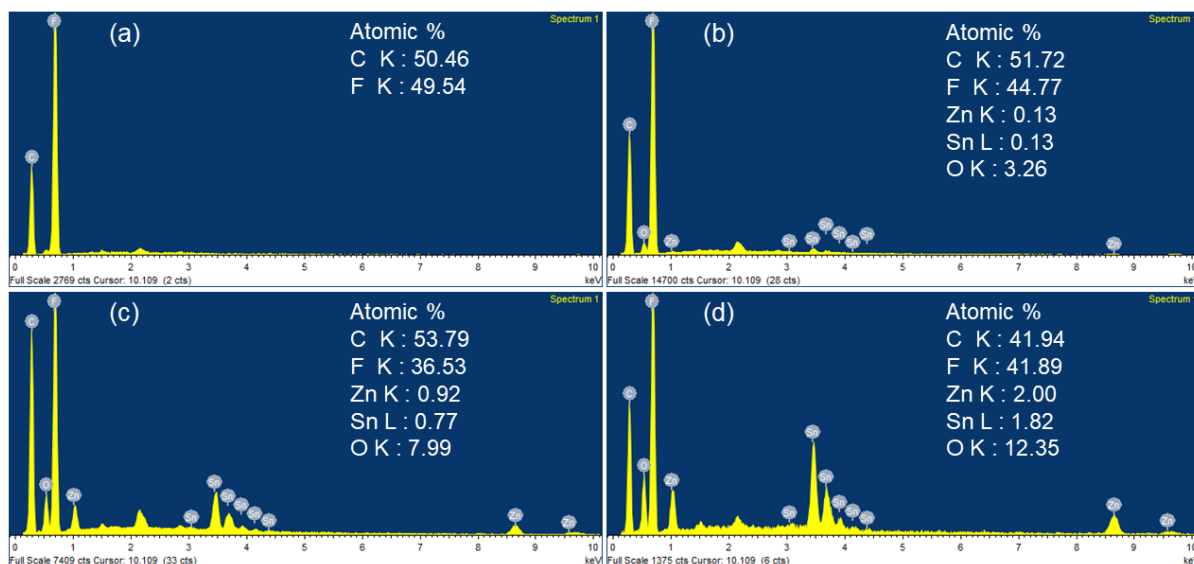


Fig. S2. EDX spectrum of (a) PTr, (b) PTr-1ZS, (c) PTr-5ZS, and (d) PTr-10ZS composite films.

Fig. S3

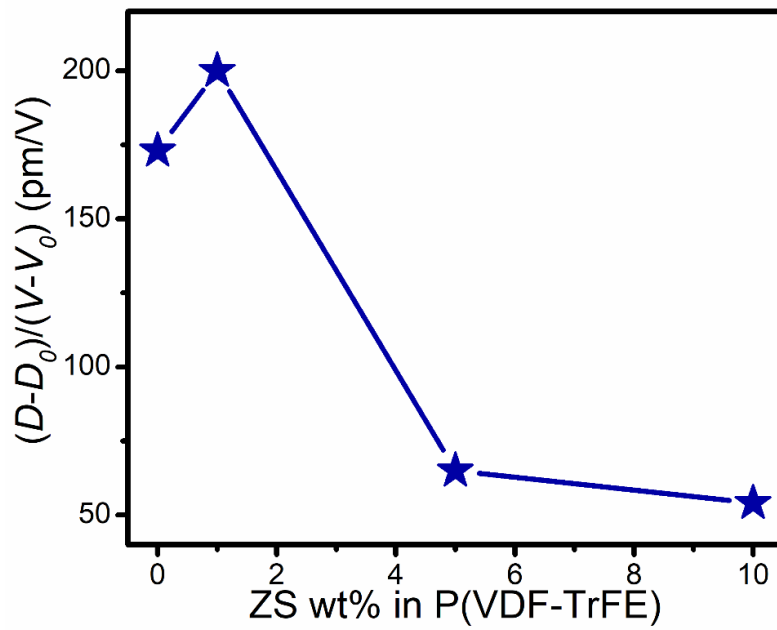


Fig. S3. Variation of absolute value $(D-D_0)/(V-V_0)$ at maximum applied tip bias of 20 V with the variation of ZS wt% in P(VDF-TrFE).

Fig. S4

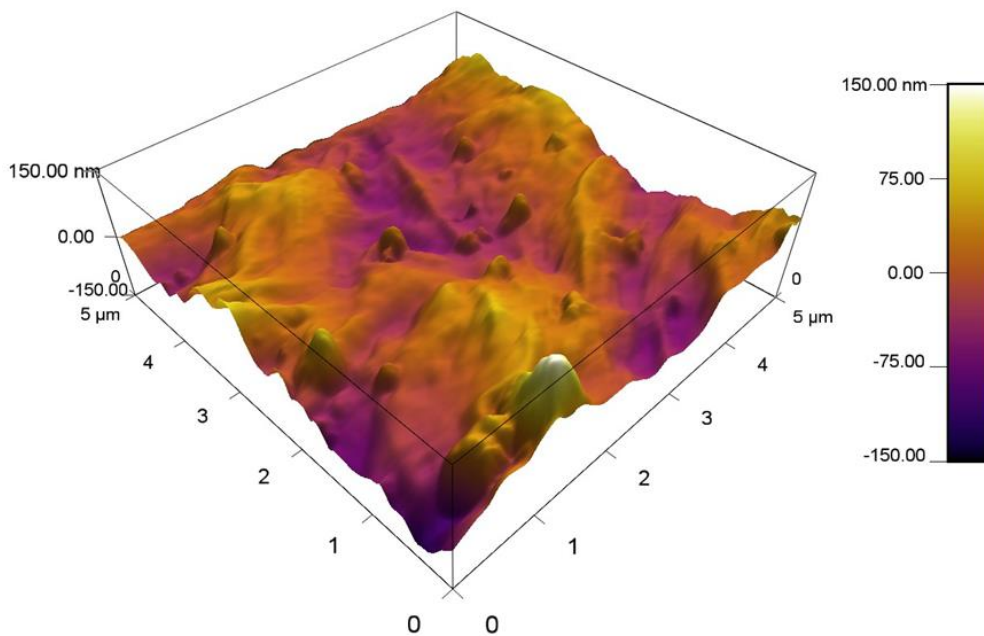


Fig. S4. The 3D topography image of the PTr-1ZS sample for a scanned area of $5 \mu\text{m} \times 5 \mu\text{m}$ obtained from PFM instrument.

Fig. S5

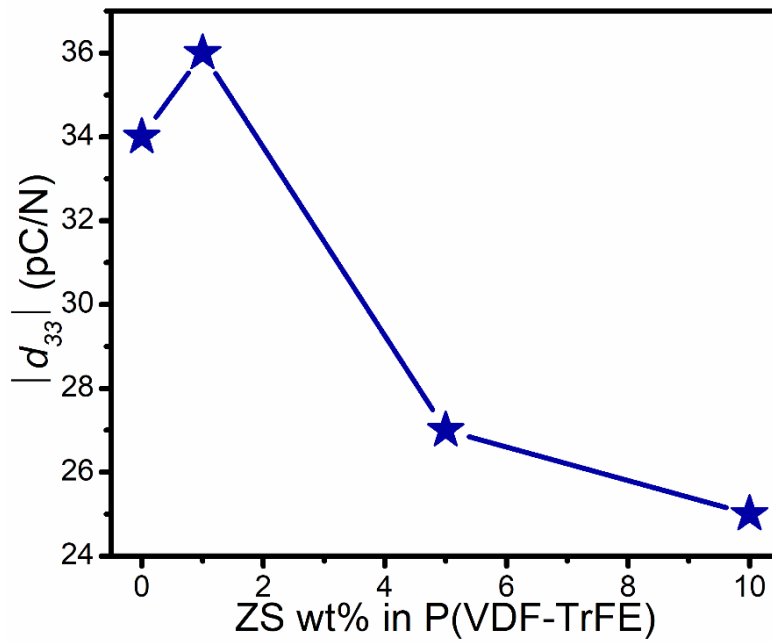


Fig. S5. Variation of $|d_{33}|$ of the composite films with the variation of ZS wt% in P(VDF-TrFE).

Fig. S6

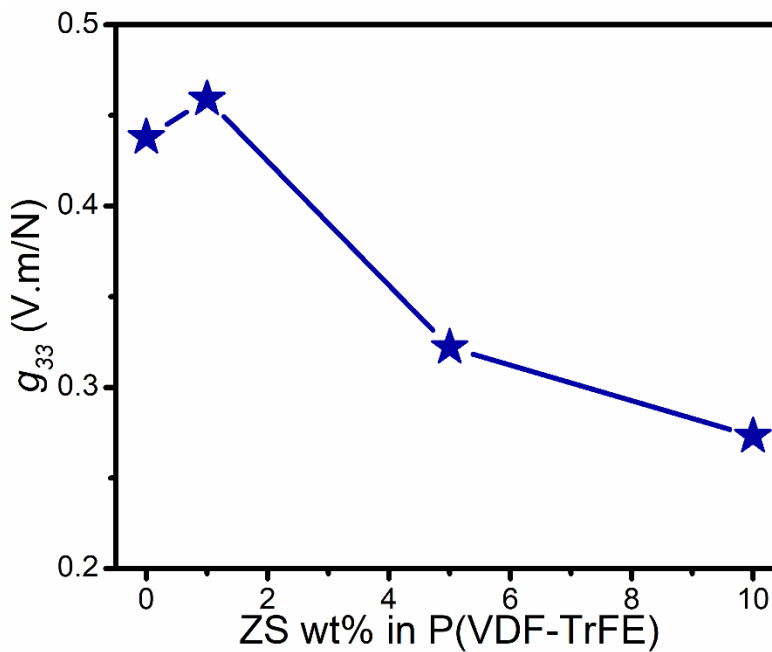


Fig. S6. Variation of g_{33} of the composite films with the variation of ZS wt% in P(VDF-TrFE).

Fig. S7

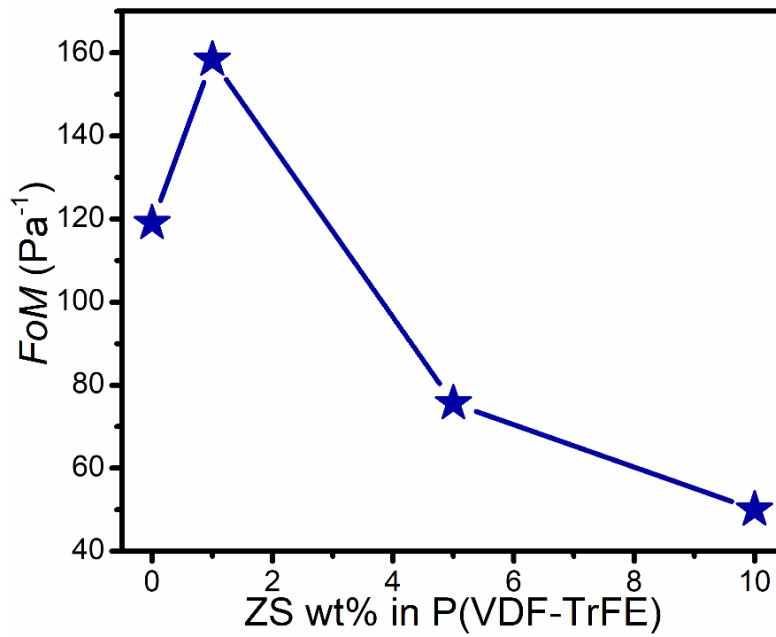


Fig. S7. Variation of FoM of the output performance of PTr/ZS based PENGs with the variation of ZS wt% in P(VDF-TrFE).

Fig. S8

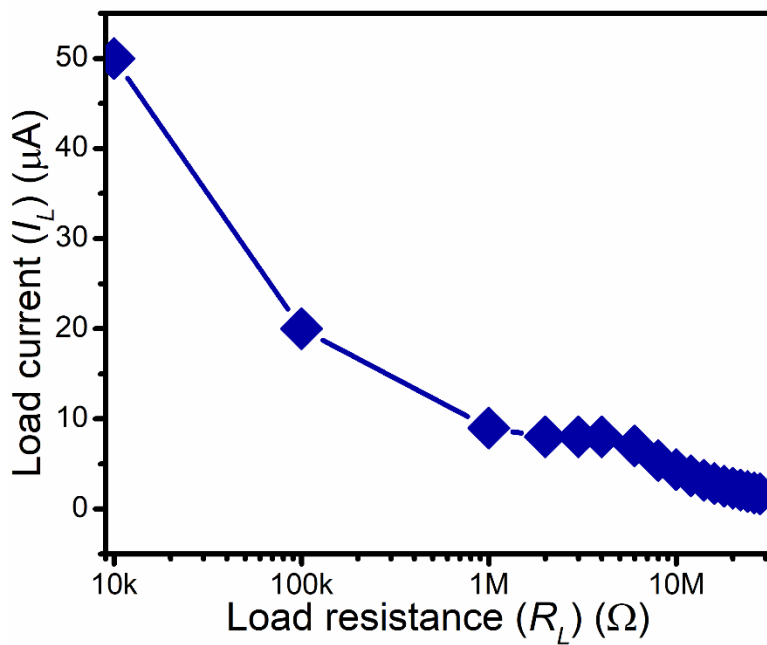


Fig. S8. R_L dependence of load current (I_L).

Fig. S9

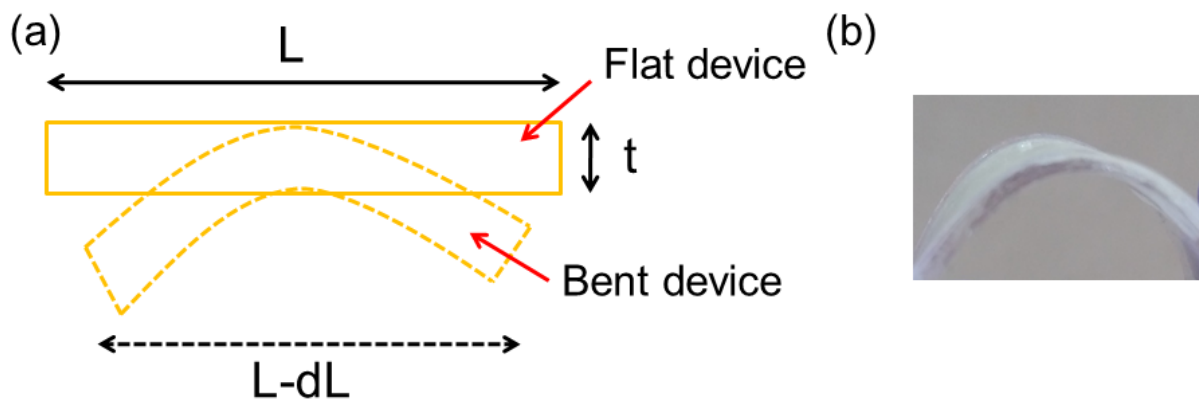


Figure S9. (a) Scheme of bending geometry and (b) digital photograph of the bent device (t = thickness, L = length, and $L-dL$ = length after deformation of the device).

Note S1

Applied input mechanical strain calculation for bending experiment

As shown in Figure S8, the two edges of the device (two opposite edges of its length) were held and bending was applied along the out-of-plane direction. If ' L ' and ' t ' be the length and thickness of the device and ' $L-dL$ ' be the thickness after deformation, then the input mechanical strain (ϵ) can be calculated by using the equation given below.

$$\epsilon = \frac{t}{2R_0} \times 100\% , \text{ where } 'R_0' \text{ is the radius of curvature after bending and is given by } R_0 = \frac{L}{2\pi\sqrt{\frac{dL}{L} - \frac{\pi t^2}{12L^2}}}$$

For the present case, the values of ' dL ' were found to be 0.2, 0.4, and 0.8 cm for three different orders of bending. By using the values of other parameters (as already mentioned in the article), the values of ' R_0 ' and ' ϵ ' were found to be 1.88, 1.31, and 0.93 cm and 6.6, 9.5, and 13.4%, respectively.

Fig. S10

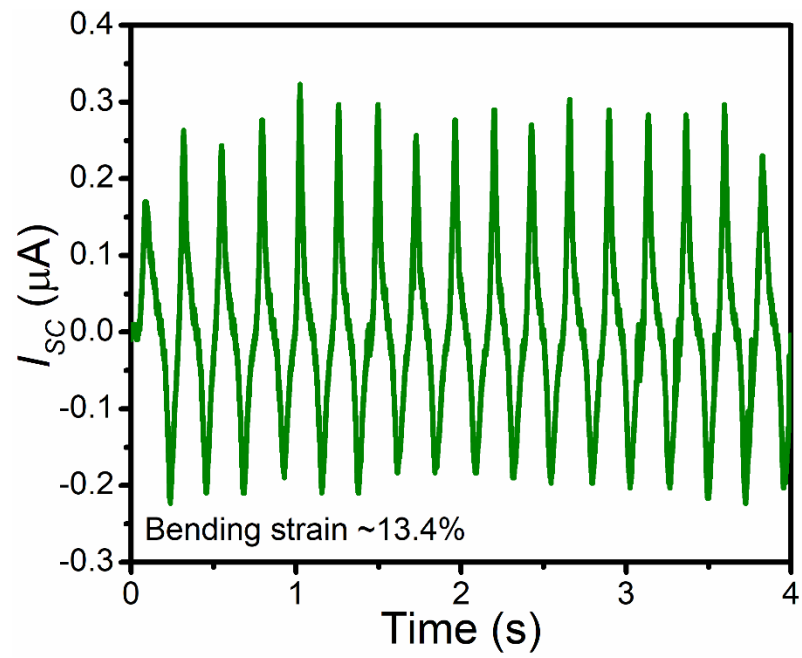


Fig. S10. Typical output I_{sc} signal from the PTr-1ZS based PENG for the applied bending strain of ~13.4%.